PRAMANA
— journal of
physics

Vol. 71, No. 6
December 2008
pp. 1321–1333

Design, construction and characterization of the compact ultrafast terahertz free-electron laser undulator

B BISWAS[1,*], V KUMAR[1], S CHOUKSEY[2] and S KRISHNAGOPAL[3]
[1]Beam Physics and FEL Lab., [2]Indus Operations and Accelerator Physics Design Division, Raja Ramanna Centre for Advanced Technology, Indore 452 013, India
[3]Nuclear Physics Division, Bhabha Atomic Research Centre, Mumbai 400 085, India
[*]Corresponding author. E-mail: bbiswas@cat.ernet.in

MS received 23 April 2008; accepted 27 May 2008

Abstract. A compact ultrafast terahertz (CUTE) free-electron laser (FEL) is being developed at the Raja Ramanna Centre for Advanced Technology (RRCAT), Indore. The undulator required for the CUTE-FEL has recently been developed. We have designed, built and characterized a variable gap, 5 cm period, 2.5 m long pure permanent magnet undulator in two identical segments. The tolerable error in the magnetic field was 1% in rms, and we have measured it to be 0.7%. The obtained rms phase shake is around 2°. To ensure that the trajectories do not have an exit error in position or angle, corrector coils have been designed. Shimming coils have been applied for both the undulator segments to reduce the amplitude of the betatron oscillations in the vertical trajectory. Details of novel corrector coils and soft iron shims are given and their performance is discussed.

Keywords. Undulator; free-electron laser; beam wander; phase shake; shimming.

PACS Nos 52.59.Rz; 41.85.Ja; 85.70.Ay

1. Introduction

The free-electron laser (FEL) is known to be a versatile source of coherent tuneable radiation at long as well as short wavelengths. In an FEL, as shown in figure 1, a high quality relativistic electron beam is injected into a magnetic structure called the undulator, where the electrons oscillate and emit spontaneous radiation. In the oscillator configuration, this radiation is trapped in a resonator cavity where it repeatedly interacts with the subsequent electron bunches, which consequently develop microbunching at the radiation wavelength [1]. As a result of this microbunching, stimulated emission is generated and the radiation becomes coherent. The wavelength of the radiation can be broadly tuned by changing the magnetic field inside the undulator and also by changing the energy of the electron beam.

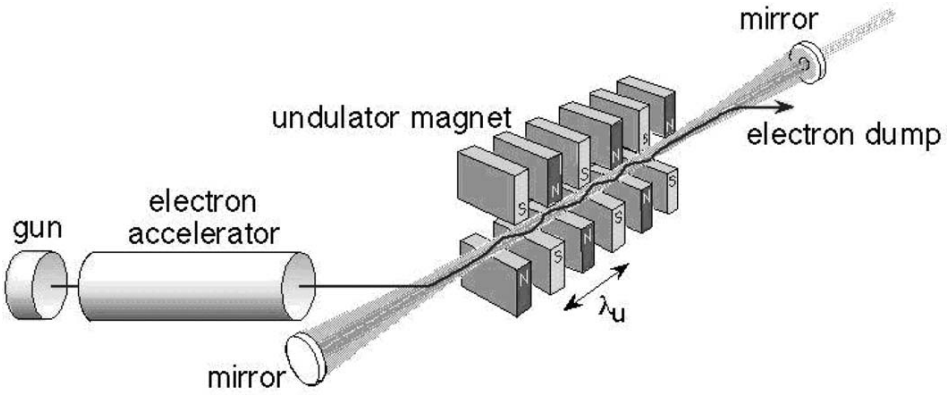

Figure 1. The schematic of an FEL oscillator.

Free-electron lasers are becoming popular at long wavelengths, where they hold the promise of filling the terahertz gap, which is a relatively unexplored area in the electromagnetic spectrum so far. On the other hand, at short wavelengths, FELs are very promising as fourth-generation light sources, where one can generate high power ultra-short pulses of coherent X-rays for research in many areas of science, such as imaging/holography of biomolecular structures, warm dense matter, femtochemistry, etc.

While an X-ray FEL requires a very high energy, bright electron beam, the electron beam requirements for a long wavelength FEL are modest. Typically a few tens of MeV of electron beam energy and few tens of Amperes of electron beam peak current are required for a long wavelength FEL, whereas an X-ray FEL requires few GeV of electron beam energy and few kilo Amperes of peak electron beam current.

At RRCAT, we are building a compact ultrafast terahertz free-electron laser (CUTE-FEL) [2]. This is an FEL oscillator, designed to lase in the terahertz region, between 100 and 50 μm, using an electron beam of energy 8–15 MeV. The electron source is a 90 kV thermionic gun. The 1 nC, 1 ns, 36.62 MHz beam from the gun is first bunched in a 476 MHz subharmonic pre-buncher, and then in a 2856 MHz buncher, before being accelerated to the required energy in a plane wave transformer (PWT) linac that we have developed in-house [3]. The peak (micropulse) current from the linac is 20 A.

This beam will be injected into a contiguous two-segment pure permanent magnet planar Halbach undulator that has a period of 50 mm and a total length of 2.5 m. The NdFeB (neodymium iron boron) magnets have a 12.5 mm square cross-section and are 50 mm long. The optical cavity will be 4.1 m long, near-concentric, with radiation out-coupled through a hole in one of the (gold-plated, copper) mirrors. The radius of the downstream mirror is 2.25 m, and that of the upstream one is 2.5 m. Radiation is out-coupled through a 2 mm radius hole in the downstream mirror. A lay-out of the CUTE-FEL is shown in figure 2.

In this paper we describe the indigenous development of the undulator for the CUTE-FEL. This is the first high-quality, variable-gap, undulator in the country.

In §2–4 we give details of the physics and engineering design of the undulator. In §5 we present results from field mapping of the undulator. This includes improvements made through the use of corrector coils and magnet shimming, discussed in some details in §6.

2. Physics design of the undulator

The design parameters of the undulator are listed in table 1. Detailed design simulations of the CUTE-FEL were performed, using the codes TDAOSC and GINGER [4–6], to determine the parameters of the undulator. The period length λ_u has been chosen to be 50 mm such that one can generate 80 μm radiation with a peak undulator parameter K of 0.8, using a 10 MeV electron beam.

Simulations show that the (2σ) optical beam diameter inside the undulator could be as large as 8–10 mm. Hence, in order to avoid significant diffraction loss, we have chosen the vacuum pipe ID to be 28 mm. The number of periods has been chosen to be 50 such that one gets enough gain inside the undulator – the small signal gain is around 36% and the cavity round trip loss is around 15%, as calculated using GINGER.

One of the constraints in designing an undulator for FEL applications is that the rms error $(\Delta B/B)_{\mathrm{rms}}$ in the amplitude of the sinusoidal field should be small enough so that the resulting inhomogeneous broadening in the gain spectrum is less than its natural width $(1/2N_u)$. This is to ensure that the gain does not reduce significantly, and leads to the tolerance condition [7]

$$\frac{\Delta B}{B_{\mathrm{rms}}} < \left(\frac{2+K^2}{4K^2N_u}\right).$$

Here K is the undulator parameter, related to the peak sinusoidal magnetic field B, and given by

$$K = \left[\frac{eB\lambda_u}{2\pi mc}\right].$$

For the design parameters of table 1, we get $(\Delta B/B)_{\mathrm{rms}} < 2\%$. However, considering that a similar gain reduction could also result due to energy spread, transverse emittance etc., we have chosen the acceptable tolerance to half of this value, i.e. 1%. For pure permanent magnets with remanant field B_{r}, the dependence of peak magnetic field B on the gap g of the undulator is given by [8]

$$B = 1.43B_{\mathrm{r}}\exp(-\pi g/\lambda_u).$$

From the above formula, we find that in order to maintain a tolerance of 1% on the peak magnetic field, one needs to maintain a tolerance of 160 μm on the undulator gap.

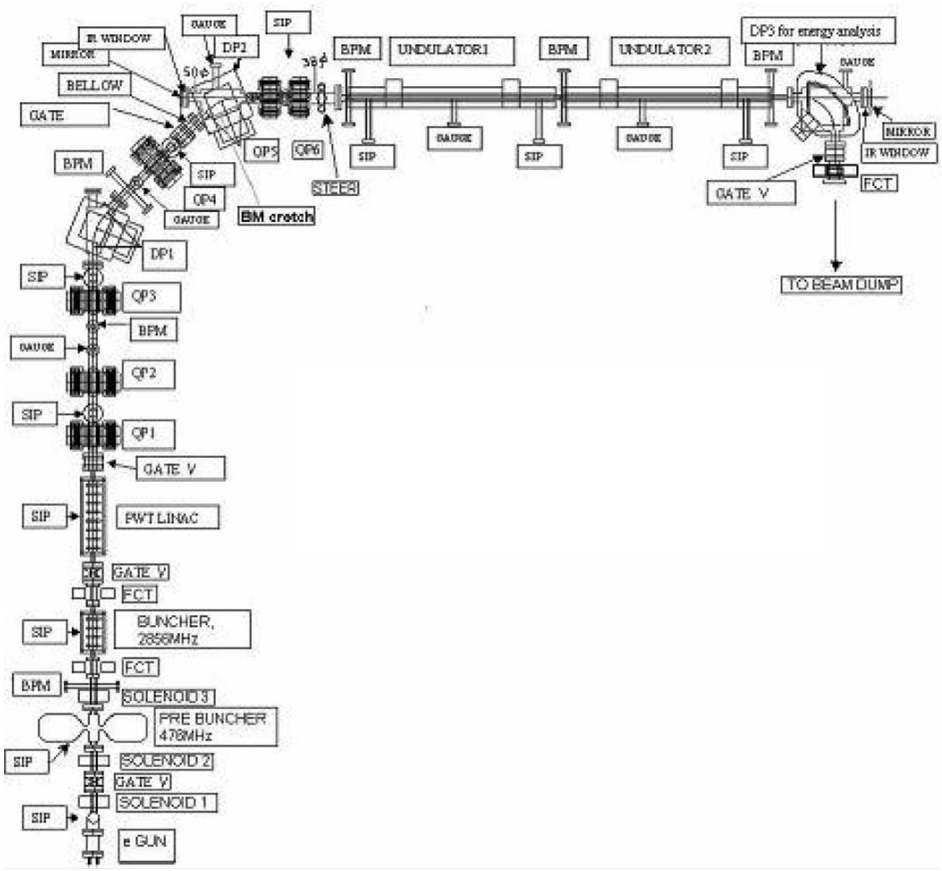

Figure 2. The lay-out of the CUTE-FEL.

Table 1. Undulator design parameters.

Parameter	Value
Type	Pure permanent magnet
Configuration	Planar, Halbach
Period length (λ_u)	50 mm
K parameter (peak)	0.8 at 35 mm gap
Magnet size	$12.5\times12.5\times50$ mm^3
Magnet material	NdFeB
Remnant field	1.1 T
No. of periods (N_u)	50
Mechanical gap	Variable, 16–100 mm
FEL design gap	35 mm

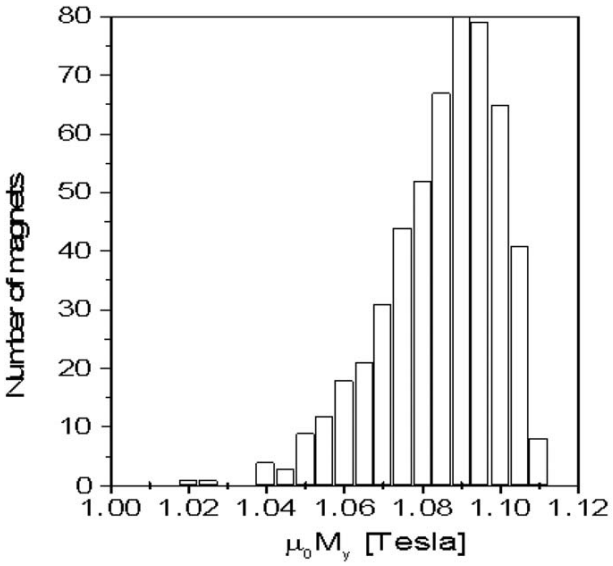

Figure 3. Histogram for M_y of the blocks.

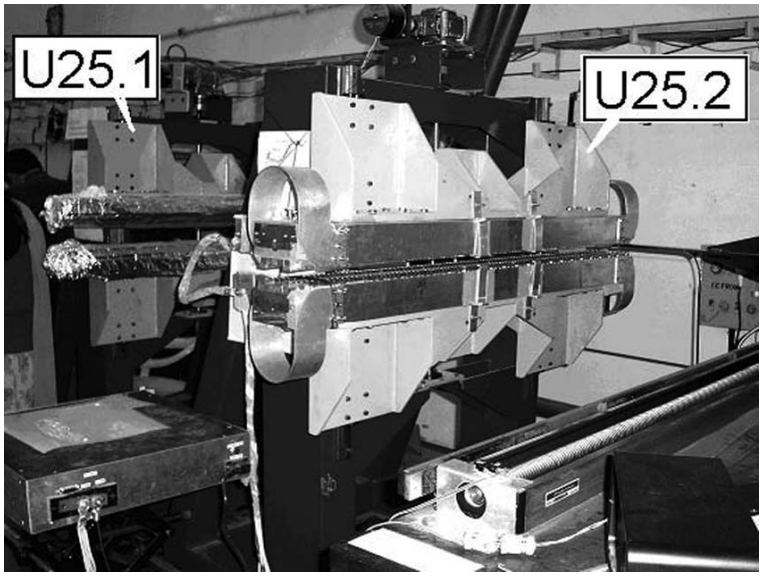

Figure 4. The undulator U25.2 (in front with corrector coil) and U25.1 in the rear.

3. Characterization and sorting of magnets

The magnetizations of 575 NdFeB magnets were measured in two dimensions (M_y, M_z) only, limited by a two-axis motion measurement set-up [9]. (The z-axis is longitudinal, y-axis is vertical and x-axis is horizontal.) The magnets were 12.5 mm square in the x–y plane, and 50 mm long. The choice of length in z was based on an estimate that, at 35 mm gap the B_y field on the axis of undulator saturates at this magnet length, which is also equal to the period of the undulator.

Figure 3 shows the histogram for M_y. We find that the mean value of $\mu_0 M_y$ is 1.085 T, with a standard deviation of 0.015 T (1.4%). We also measured the tilt of the magnetization vectors from the y-axis (in the y–z plane) and found them to lie between ±200 mrad. Obviously, it was not possible to use these magnets directly to achieve the tolerance limit of better than 1% in the peak field. In order to reduce the field error we have used the numerical technique of simulated annealing [10] to determine a particular arrangement of these magnets in the undulator that gives the minimum error. Using this technique we reduced the theoretical error to 0.4%. The errors due to misalignments, i.e., variation in position and angle of each individual magnets, further add to the theoretical number of 0.4%.

4. Mechanical design and fabrication

The undulator uses a total of 400 NdFeB magnets, leading to large static forces between these magnets. The magnets had to be arranged in a row, with positional tolerances better than 50 μm. Therefore, it was extremely important to calculate the total forces, and develop a robust structure capable of withstanding these forces. The structures of the two undulators are shown in figure 4.

For the parameters mentioned in table 1, we found that the force acting on the individual magnets, when assembled in the undulator, was about 350 N. The attractive force between the jaws was found to vary between 660 N at a gap of 30 mm, to 8000 N at 10 mm gap. The mechanical design was such that one can safely lower the gap to 16 mm and the maximum deflection in the structure is less than 10 μm at any gap. Based on these considerations we designed the magnet clamping mechanism, undulator jaws and the support structure with a variable-gap drive mechanism [11]. In order to achieve the required parallelism between the two jaws while varying the gap, we used a linear-bearing based guiding system. A precision-grade double-acting grounded ball screw was used to ensure the required positional accuracy.

The material for the magnet block camps and period holders was chosen to be stainless steel, AISI grade SS316L. For the jaws we chose SS304. The material of the support structure was chosen to be mild steel (MS). Thickness of the jaw was chosen such that any MS component was at a sufficiently large distance from the magnets to prevent field deterioration by magnetization of MS. During the process of fabrication of these components, we often encountered the problem that the SS components used to get magnetized after machining. We got around this problem by solution annealing these components in a vacuum furnace at a temperature of 1,200°C for about 2 h, and then rapidly cooling them. In this way we could

Table 2. Parameters of undulators U25.1 and U25.2.

Parameter	Design goal	U25.1 Actual	U25.2 Actual
Error in peak field (rms)	$< 1\%$	0.9%	0.7%
Error in period (rms)	< 100 μm	82 μm	85 μm
Phase shake (rms)	$< 3^\circ$	2°	2°
Beam wander (rms)	< 0.5	1.6	0.33
wiggle-amplitude		0.14 (with shims put in place)	0.10 (with shims by simulation)

reduce the relative permeability to less than 1.01. After these components were fabricated, we assembled the magnets as per the arrangement calculated by the simulated annealing procedure mentioned in the last section. It was required to assemble the magnets with a gap less than 10 μm between adjacent magnets and it was confirmed by checking with a 10 μm aluminium foil.

To do the magnetic field mapping of this undulator, we have developed a simple magnetic field mapping system that consists of a Hall probe mounted on a three-axis linear motion system. The entire system has been mounted on a heavy granite table. The running parallelism of the linear motion system is ± 0.02 mm as checked with a dial gauge. The distance along the undulator axis was recorded using linear optical encoder having an accuracy of 0.02 mm as checked with a laser interferometer.

We have also used this linear motion system to align the undulator by mounting the base of the dial gauge on a bracket bolted to the motion system and letting its non-magnetic dial tip touch the magnet surface. The rms variation in the gap between the two jaws along the length of the undulator has been measured to be 40 μm. This is within the tolerance limit of 160 μm discussed in §2.

5. Field mapping and trajectory calculation

The two undulator sections, U25.1 and U25.2, shown in figure 4, were field mapped using a miniature 3-axis Hall effect teslameter (Senis make-3MH2-A2D3-2-2T, field sensitive volume 0.01 mm^3) [12]. The designed and measured parameters of U25.1 and U25.2 are given in table 2, at a gap of 35 mm. For good electron beam–radiation interaction, the electron beam needs to be confined in a narrow envelope that is fully immersed in the envelope of the cavity radiation. This is usually qualified by rms of transverse positional excursion of electron beam from axis, normalized to the nominal wiggle amplitude – called beam wander.

Similar variation of the phase of the electron wiggle is called phase shake, which is strongly correlated to the FEL gain as shown by Bobbs *et al* [13]. We report in table 2 that the tolerances on errors in the period, peak field and phase have all been met.

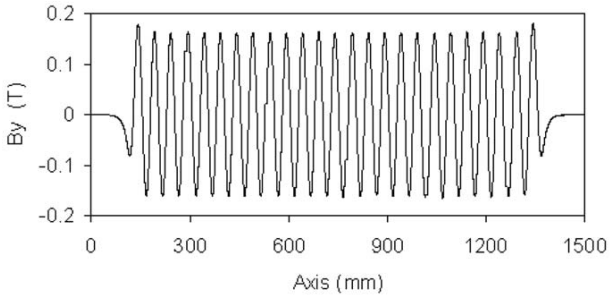

Figure 5. Field B_y on the axis of U25.1.

5.1 *Vertical field and horizontal trajectory*

The mapped vertical field of U25.1 is shown in figure 5, and it is indistinguishable from that of U25.2, which is hence not shown. For U25.1 and U25.2 the calculated horizontal trajectories [14] of a 10 MeV electron beam, obtained from the second integrals of the vertical field B_y, are shown in figures 6a and 6b respectively. It is seen that the horizontal trajectories have a net exit error in position and angle.

In U25.1, there is need for a constant 2.5 G vertical field correction (sometimes also called compensation as this correction is done over the full undulator length) along with a shim (that adds a small corrective field $B_{\text{y-shim}}$ locally), in order to straighten the horizontal trajectory as well as to remove positional offset and angle at the exit. A calculation was done for vertical field shimming in U25.1. The field signature of the shim at an undulator gap of 35 mm is shown in figure 7 and again shown in figure 6a for specifying the location of the shim. Multiple strips of high nickel steel, of 100 μm thickness, have been used for shimming. The first field integral of the shim is 30.8 G-cm. After shimming, U25.1 was mapped again. The measured first field integral of the shim agrees well with that by simulation. The corrected horizontal trajectory is also shown in figure 6a. It can be seen that there is a further improvement in the trajectory as a consequence of the shimming – the beam wander is reduced from 1.6 to 0.14 wiggle amplitudes.

Any shimming procedure should not affect the periodicity of the undulator field. We have seen that the rms phase shake of 2° in U25.1 is unaffected by shimming. We found that shims having chamfered corners were much more stable against slipping to either side of the permanent magnet bed.

In U25.2 a constant 0.5 G vertical field correction (or compensation) is enough to both straighten the horizontal trajectory and remove exit positional error from the principal axis. For U25.2, the beam wander of 0.33 is already less than the maximum acceptable value of 0.5, hence shimming has not been implemented on the device. However, as U25.2 was mapped earlier than U25.1, at that stage a finer shimming calculation was done for U25.2, to further improve the horizontal trajectory and reduce the beam wander to less than 0.1 [15].

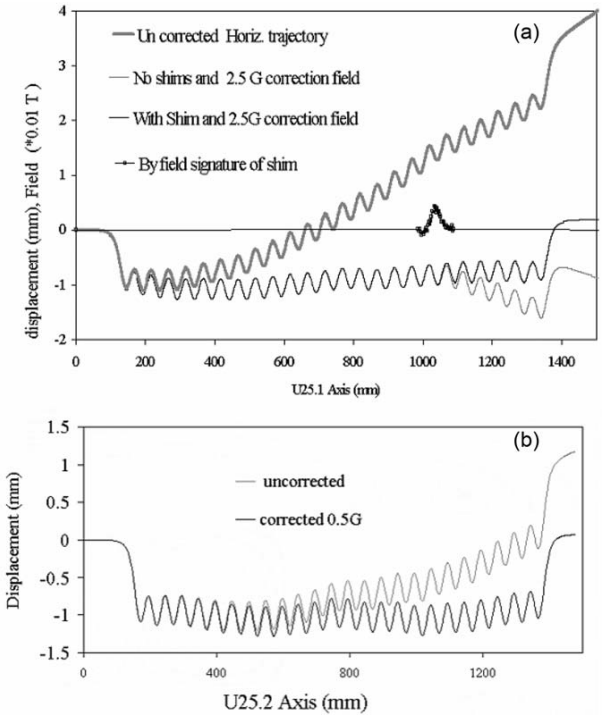

Figure 6. (**a**) Horizontal trajectory for U25.1, as mapped, with 2.5 G compensation without shims, and with 2.5 G compensation and shim. The shims' location and magnetic field signature (ordinate field scale $\times$ $10^{-2)}$ is also shown. (**b**) Horizontal trajectory for U25.2 as mapped, and with 0.5 G compensation.

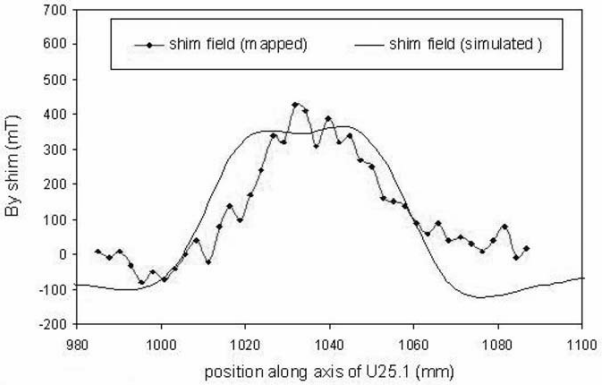

Figure 7. The mapped and simulated field signatures of ferromagnetic shim used in U25.1. Both have 30.8 G-cm first field integral. The same field signature is also shown earlier in figure 6a, at the axial position where it is put inside U25.1.

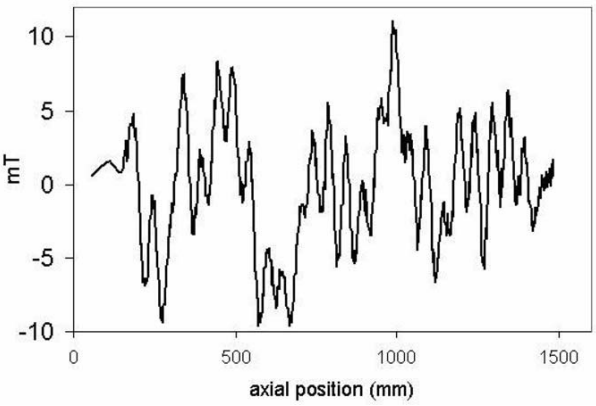

Figure 8. The mapped on-axis horizontal field B_x in undulator U25.2.

5.2 *Horizontal field and vertical trajectory*

For calculating the vertical trajectory through the undulator, the horizontal transverse field B_x was measured using the 3-axis Hall probe as shown for U25.2 in figure 8. For U25.1 and U25.2, the calculated (10 MeV) electron beam vertical trajectories, based on the mapped field B_x, are shown in figures 9a and 9b respectively. The focussing by the undulator in the vertical plane was included [16].

Even after trajectory straightening (compensation), using horizontal field (B_x) corrector coils along the full length of the undulator, there was significant beam-wander in the vertical plane. To correct this we have put local 'shim coils' that generate opposite $\int B_x \, \mathrm{d}z$. The hard-edge shim coil B_x field profiles are also shown in these figures, which reduce the beam excursion to within $+/-0.5$ mm in the vertical. This is important as the undulator's sinusoidal peak field B_y increases hyperbolically in y – the vertical distance from the axis.

6. The design of corrector and shim coils

For the vertical field compensation we have built racetrack-type rectangular coils (with saddle-type ends), which can generate up to 5 G field over the full length of the undulator. The vertical field corrector coils (shown in figures 4 and 10) have been designed to provide up to 5 G vertical field with $\Delta B/B$ better than 0.8% in a 10 mm diameter bore about the axis of the undulators, and at a gap of 35 mm. In this case there was no space available to put a four-wire type magnet coil, as we have used that space for horizontal field corrector coils. The mapped field of the vertical corrector coil along with the vertical sinusoidal field in U25.2 is shown in figure 11. The hard edge field integral due to the vertical corrector coils is $\sim$0.5 G $\times$ 2.5 m. The corrector coils have a zero fringe field region outside their physical edge. This has been done so that the two undulator segments can be placed contiguously.

For corrections in the horizontal field we have used four-wire type magnet coils as shown in figure 10. The horizontal field corrector coil (to generate 0–5 G) extends

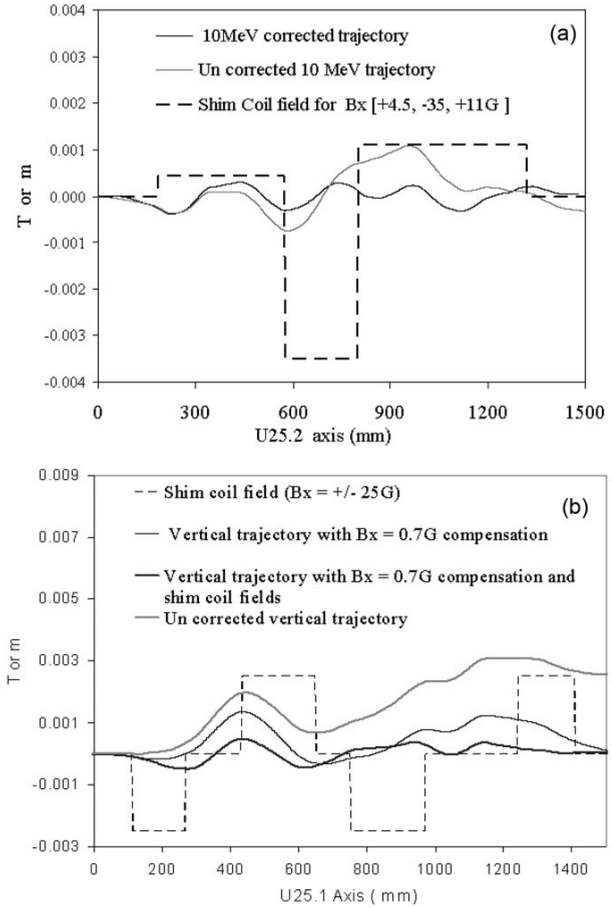

Figure 9. (**a**) Vertical trajectory through U25.1, with 0.7 G compensation and with/without shim coils in place. (**b**) Vertical trajectory through U25.2 with/without shim coil in place. The shim coil fields and their locations are also shown.

over the full length of undulator. The horizontal field 'shim coils' (to generate 0–40 G) are placed at desired locations along the undulator.

Ferromagnetic strip shims are usually used for shimming the B_x field, but the corrections are usually small – up to a few Gauss. If ferromagnetic shims are used to vary the B_x field by $+/-20$ G, then the peak field B_y at that same location is also perturbed by more than 1% from its design value (1,690 G at 35 mm gap). In our case the effective corrections in B_x are about 15 to 45 G. Hence, we shall use electromagnetic shim coils to generate local fields up to 50 G in the x direction. There is very little clearance available to accommodate the horizontal corrector/shim coils between the two jaws of the undulator. The shim coils have to be a single-turn water-cooled type electromagnet. The locations for the shim coils are optimized for minimum $\Delta B/B$ in B_x.

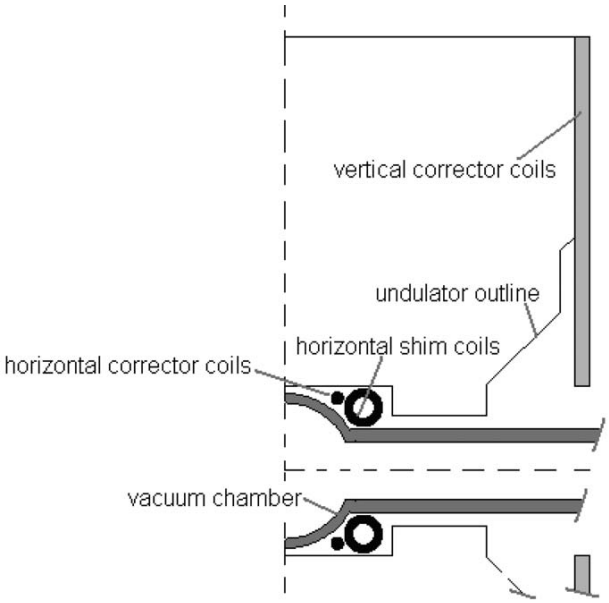

Figure 10. Sectional view of the vertical corrector coils (plate type), horizontal corrector/shim coils (four wire type) and vacuum vessel.

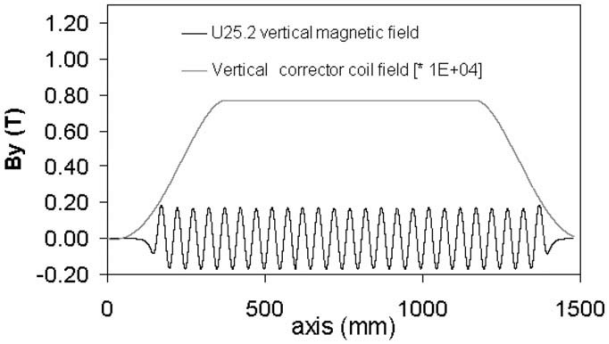

Figure 11. The vertical corrector coil field and the vertical field in U25.2 along the axis of undulator.

7. Conclusion

We have built the first high-quality, variable-gap undulator in the country. The twin undulator segments developed in-house meet their design goals for lasing the CUTE-FEL at 80 μm. In order to ensure no degradation in FEL gain, the beam–radiation overlap needs to be as good as possible. This translates to further straightening of the trajectories and reducing local beam excursions from the principal axis. Corrector coils for horizontal and vertical fields have been designed for this purpose.

Soft-iron shimming has been employed to improve the rms beam wander in the horizontal trajectory. The beam wander in U25.1 was reduced from 1.6 to 0.14. In U25.2 the rms beam wander is 0.33 and is already acceptable.

Local shim coils (electromagnets) have been designed to locally offset the uncompensated random horizontal field in the undulator by up to 50 G and reduce the beam's trajectory wanders in the vertical field to within acceptable limits. We have recently completed construction of the vacuum pipe for transmission of electron beam through the undulators.

References

[1] S Krishnagopal, V Kumar, S Maiti, S S Prabhu and S K Sarkar, *Curr. Sci.* **87(8)**, 1066 (2004)

[2] S Krishnagopal, B Biswas, S Chouksey, S K Gupta, U Kale, A Kumar, V Kumar, S Lal, P Mehta, P Nerpagar and K K Pant, *Proceedings of FEL Conference* 496 (2006)

[3] A Kumar, K K Pant and S Krishnagopal, *Phys. Rev. ST Accel. Beams* **5**, 103501 (2002)

[4] T M Tran and J S Wurtele, *Comput. Phys. Commun.* **54**, 263 (1989)

[5] S Krishnagopal, M Xie, K-J Kim and A Sessler, *Nucl. Instrum. Methods in Phys.* **A318**, 661 (1992)

[6] W Fawley, *A user manual for ginger and its post-processor* XPLOTGIN, LBNL-49625-Rev.I ed., Lawrence Berley National Laboratory (2004)

[7] J B Murphy and C Pellegrini, in: W B Colson, C Pelligrini and A Reneiri (eds), *Laser handbook* (Elsevier Science Publishers B.V., The Netherlands, 1990), Vol. 6

[8] C A Brau, *Free-electron lasers* (Academic Press Inc., San Diego, 1990) p. 263

[9] V Kumar, M R Jathar, V Meshram and A Verma, Characterisation of Nd–Fe–B magnets for FE undulator, *DAE Solid State Physics Symposium* (Kurukshetra, Dec. 27–31, 1998) pp. 225–226

[10] A D Cox and B P Youngman, *Proc. SPIE* **582**, 91 (1985)

[11] Sanjay Chouksey, V Kumar and S Krishnagopal, Mechanical design and fabrication of pure permanent magnet undulators, *Indian Particle Accelerator Conference – 2003* (InPAC-2003) (CAT, Indore, Feb. 3–6, 2003)

[12] Senis Gmbh, http://www.senis.ch (Earlier known as Sentron Gmbh)

[13] B L Bobbs *et al*, *Nucl. Instrum. Methods in Phys.* **A296**, 574 (1990)

[14] Xie Jialin *et al*, *Nucl. Instrum. Methods in Phys.* **A304**, 770 (1991)

[15] B Biswas, V Kumar, S Krishnagopal, K K Pant, S Lal, U Kale, P Nerpagar, InPAC-2005, 89–90, VECC Kolkata, March 1–5, 2005

[16] C A Brau, *Free-electron lasers* (Academic Press Inc., San Diego, 1990) p. 155